Silicon photodiode device with 100% external quantum efficiency

Edward F. Zalewski and C. Richard Duda

A device utilizing four inversion layer photodiodes in a light-trapping arrangement was constructed and tested. The device was found to have a photon-to-electron conversion efficiency of 0.999 for short wavelength and low power visible radiation. It was found that applying a reverse bias voltage extended the high quantum efficiency response over the entire visible spectrum and up to the highest radiant power level studied (several milliwatts). Several radiometrically important characteristics were studied and the results presented: spectral reflectance; polarization sensitivity; quantum efficiency vs wavelength, photon flux density, and reverse bias voltage; and dark current vs reverse bias.

I. Introduction

A technique for predicting the external quantum efficiency (photon-to-electron conversion efficiency) of a silicon photodiode in the 380–900-nm spectral region was developed recently and demonstrated to be very accurate[1,2] and quite simple[3] compared with conventional thermal radiometric techniques. For the photodiodes used in those studies the principal loss mechanisms in the photon-to-electron conversion process are the loss of photons due to reflection at the front surface and the loss of minority carriers due to recombination. Recombination losses can be characterized by the three regions in which they occur: (1) at the SiO_2–Si interface; (2) in the front volume between the interface and onset of the depletion region; (3) in the rear volume outside the depletion region. Recombination losses in Region 1 can be measured by the oxide bias method.[4] In Region 2 the recombination losses are small and can be neglected except at short wavelengths.[2] In Region 3 it has been shown that recombination losses can be eliminated by applying a reverse bias voltage[4] to extend the depletion region.

It has also been shown that for an inversion layer type of silicon photodiode the recombination losses at the interface and in the front volume are negligible.[5] The inversion layer silicon photodiode was developed by Hansen[6] and is now manufactured by United Detector Technology. In this type of photodiode the junction is induced in the Si by positive charges trapped in the SiO_2. The front region minority carriers (holes) are repelled from the SiO_2–Si interface by the trapped positive charge and swept across the junction by the field within the depletion region before a significant amount of recombination can occur.

For short-wavelength photons that are entirely absorbed in the front region, the only significant loss in an inversion layer photodiode is that due to reflection. With the application of a reverse bias voltage, the range over which this is true can be extended to longer wavelengths. In this paper we will describe a simple light-trapping arrangement of several inversion layer photodiodes that eliminates the loss due to reflection. The external quantum efficiency of this device has been measured and found to be 0.999 ± 0.002 in the 400–700-nm wavelength range.

Because of its potential as an absolute radiometric standard we have examined several characteristics of a small sampling of the inversion layer photodiodes used in the multiple detector devices as well as some of the characteristics of the overall device. The various characteristics studied and presented in this paper are: the geometrical properties, that is, the shape and size of the field of view of this particular configuration and its approximate relationship to the spectral variation of reflectance; the effect of the reflectance on quantum efficiency and polarization sensitivity; the wavelength variation of the quantum efficiency; the effect of reverse bias on the quantum efficiency; the effect of photon flux density on the quantum efficiency; and the effect of reverse bias on the dark current in inversion layer photodiodes with a comparison with other types of silicon photodiode. Finally, we discuss several possible improvements for future generations of multiple inversion layer photodiode devices plus a possible 100%

Edward Zalewski is with U.S. National Bureau of Standards, Washington, D.C. 20234, and C. R. Duda is with United Detector Technology, Hawthorne, California 90250.

Received 12 May 1983.

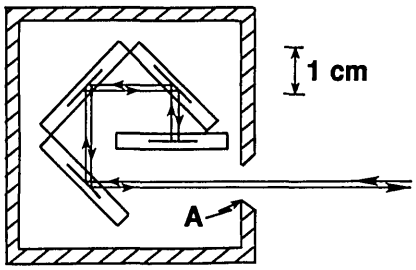

Fig. 1. Optical configuration of the four photodiodes (top). The reflected light beam is shown displaced from the incident beam for clarity of illustration.

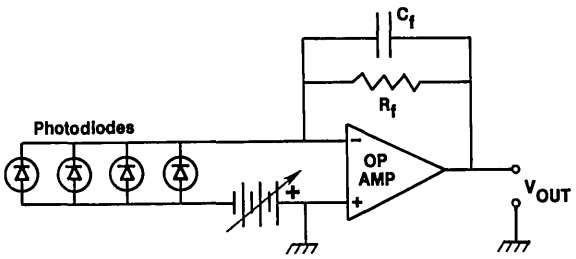

Fig. 2. Electrical configuration of the four photodiodes, dc bias, and operational amplifier.

quantum efficient device based on the more widely used p-n type of silicon photodiode.

II. Experiment

The light-trapping arrangement used in this study is illustrated in Fig. 1. Three windowless photodiodes were set at 45° to the incident radiation so that the reflected radiation from the first photodiode was incident on the second and so on. A fourth windowless photodiode was set at normal incidence so that the radiation was reflected back along the original path. The radiation, therefore, was incident on seven surfaces before exiting the device.

The active area of the silicon photodiodes was 1 cm^2 (circular). In the arrangement depicted in Fig. 1 the angle subtended by the last reflecting surface from a point on the first surface is 4.2° in the plane of the reflections and 5.9° perpendicular to this plane. For a 0.1-cm^2 aperture at the plane of the entrance to the housing (point A in Fig. 1), the field of view at 1 m from this aperture would be an ellipse with major and minor diameters of 5.0 and 2.7 cm, respectively. At 50 cm from the aperture the major and minor diameters would be 2.3 and 1.2 cm. This is the minimum field of view. Because of the lower reflectance at long wavelengths, as will be discussed later, complete absorption is accomplished in fewer than seven reflections, and in the long-wavelength region the field of view will be considerably larger.

The output currents of the four photodiodes were summed by connecting them in parallel. The total output current was measured using a low noise operational amplifier in the configuration shown in Fig. 2. The gain of the amplifier was calibrated within an uncertainty of <0.05%. A variable dc power supply was connected in series with the photodiodes to produce the reverse bias needed to restore 100% collection efficiency at high radiant flux levels and/or long wavelengths. A word of caution: depending on the dc power supply, its placement in the circuit, and the magnitude of the feedback resistor, ground loops and feedback oscillation are potential problems. Such problems can be detected by monitoring the amplifier output with an oscilloscope.

The external quantum efficiency was measured at four laser wavelengths: 406.7, 676.4, and 799.3 (krypton-ion laser), and 632.8 (He–Ne Laser) nm. These were amplitude stabilized[7] cw lasers. As a further step to improve the long-term laser stability and increase the precision of the measurements, a separate silicon photodiode was used to monitor the laser beam power and correct for residual drift.

Except for the 406.7-nm line, the laser beam power in the 1–2-mW range was measured with both a self-calibrated silicon photodiode[1,2] and an electrical substitution thermopile radiometer.[8] Because the amount of recombination occurring in Region 2 cannot be accurately estimated and, for 406.7-nm radiation, is too large to be neglected for the p-n type of photodiode used in the self-calibration, the electrical substitution thermopile radiometer was the sole absolute basis of the 406.7 nm measurement. The estimated uncertainty of the quantum efficiency as measured with either technique was ±0.2%. Both measurement methods agreed to well within the estimated uncertainties.

With a known radiant power input ϕ and measurement of the photocurrent (output current minus the dark current) I, the external quantum efficiency Q is obtained by

$$Q = \frac{I \cdot h \cdot c}{\phi \cdot n \cdot e \cdot \lambda}, \tag{1}$$

where h is Planck's constant, c is the velocity of light, n is the index of refraction of air, e is the elementary electronic charge, and λ is the wavelength of the laser radiation. In the visible region of the spectrum

$$\frac{h \cdot c}{n \cdot e} = 1.2395 \times 10^3 \text{ (W nm A}^{-1}\text{)}. \tag{2}$$

At radiant power levels below 1 mW, a p-n silicon photodiode (the type used in the self-calibration procedure) was used as the basis of the measurement. The high degree of linearity of the responsivity of these silicon photodiodes (<0.1% deviation in 8 decades) has been well verified.[9–11] The uncertainty in these measurements was dominated by the precision of the comparison between the single photodiode and the multiple photodiode device.

The photodiodes had a thermally grown SiO_2 layer on the front surface acting as an antireflection coating. The thickness of this layer was estimated by measuring at 406.7 nm the reflectance of the first photodiode in two of the multiple detector devices. This was done by measuring the photocurrent I_1 from the first photodiode by blocking the radiation from reaching the last three

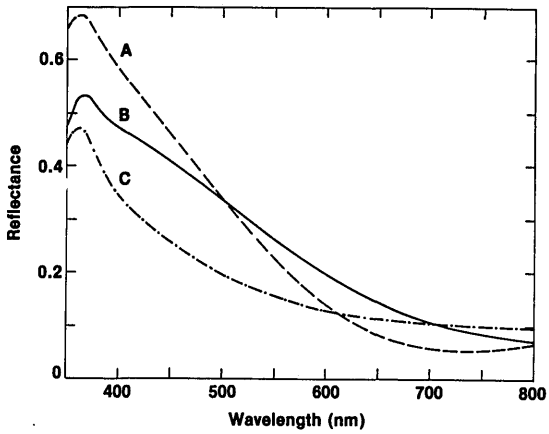

Fig. 3. Spectral variation of the reflectance of a 140-nm thick layer of SiO_2 on Si: *A*, TE polarized 45° angle of incidence; *B*, 0° incidence; *C*, TM polarized 45° incidence.

photodiodes. Then by unblocking the beam, the photocurrent from all four photodiodes I_t was measured. Since the quantum efficiency is equal to the fraction of photons transmitted into the SiO_2 (i.e., one minus the reflectance) and if the difference in reflectance between 45 and 0° incidence is neglected, the reflectance ρ can be approximated as follows:

$$\rho \simeq 1 - (1 - \rho^7)I_1/I_t \simeq 1 - (I_1/I_t). \quad (3)$$

At other than normal incidence the reflectance varies with polarization. The photodiode reflectance was measured in both the TE (electric vector transverse to the plane of reflection) and the TM (transverse magnetic) modes. The thickness of the SiO_2 layer was calculated[12] using the real and imaginary indices of refraction[13] of Si and the real index of refraction[14] of SiO_2. For four reflectance measurements the SiO_2 thickness estimates varied from 138 to 148 nm. The nominal thickness was chosen to be 140 nm.

III. Results

Figure 3 shows the calculated reflectance of a 140-nm thick layer of SiO_2 on Si for 0 and 45° incident radiation in the 350–800-nm wavelength range. Using these reflectance values one can predict the quantum efficiency as a function of wavelength. This is shown in Fig. 4 for the detector configuration used in these experiments. It has been assumed that nonspecular reflection losses are negligible. For TM polarized radiation, the calculated external quantum efficiency is 0.999 at 406.7 nm, increasing to 1.000 within 10 nm. For radiation polarized in the TE mode, the calculated quantum efficiency at 406.7 nm is 0.986, increasing to 1.000 at 500 nm. The calculated quantum efficiency in the 350–365-nm region includes the increase of the quantum yield above unity due to impact ionization.[15]

Note that at long wavelengths the light does not have to be incident on all seven surfaces before a negligible reflection loss is obtained. For example, for unpolarized light at 550 nm a quantum efficiency of >0.999 is obtained with only five reflections. Therefore, due to the configuration of this device, the longer the wavelength the greater the field of view.

The quantum efficiency at 406.7 nm in the TM polarization was measured on two devices and found to be 0.999 for both of them. In the TE polarization the measured quantum efficiencies were 0.988 and 0.989. This is in excellent agreement with the predicted value. At 632.8 and 676.4 nm the measured quantum efficiency was 0.999, which is also in excellent agreement with the prediction. The measurements at 406.7 nm were made with a reverse bias of 10 V; at 632.8 and 676.4 nm, the reverse bias used was 20 and 40 V, respectively. A reverse bias was necessary to offset the forward bias current and to overcome the recombination trap effect, as will be discussed below. A third device that demonstrated a reasonably low dark current level at very high reverse bias was measured at 799.3 nm and found to have a quantum efficiency of 0.990 at 100 V. An extrapolation (see below) indicated that 100% quantum efficiency would be obtained at ~180-V reverse bias, which was well beyond the limits of our dc power supply.

At high photon flux levels the flow of photogenerated charge carriers in the relatively high resistance inversion layer produces a forward bias. This generates a forward current which offsets the collection current. This is the mechanism of the saturation nonlinearity in silicon photodiodes.

The recombination trap effect is related to the other type of silicon photodiode nonlinearity: suprasresponsivity. This manifests itself as an increase in quantum efficiency with increasing radiant power. It is caused by the filling of recombination traps with photogenerated minority carriers. The carriers are trapped for some time before recombination occurs, thus deactivating the site. As the recombination traps are filled the minority carrier lifetime increases, thereby increasing the number of minority charge carriers collected at the junction.

The quantum efficiency measurements reported above were made at radiant power levels of 1.6–2.2 mW

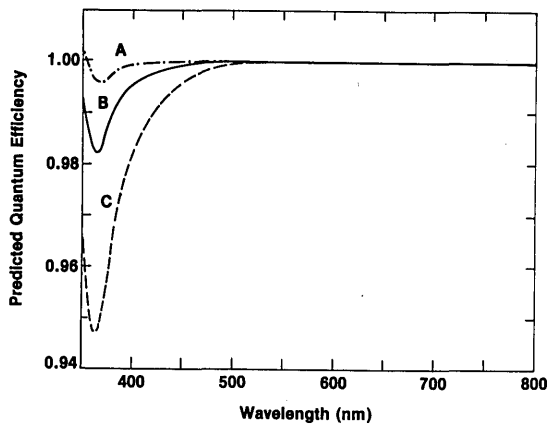

Fig. 4. Predicted quantum efficiency of the four photodiode light-trapping devices used in this study: *A*, TM polarized input; *B*, unpolarized; *C*, TE polarized.

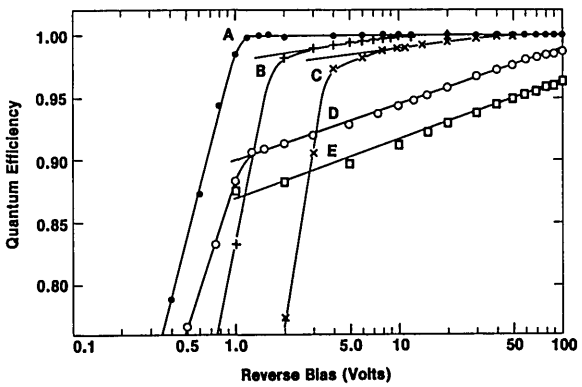

Fig. 5. Measured quantum efficiency at several wavelengths as a function of reverse bias voltage (see Table I): *A*, 406.7 nm; *B*, 632.8 nm; *C*, 676.4 nm; *D*,*E*, 799.3 nm. Curves *A*–*D* were obtained with a radiant power of ~2 mW, *E*, ~20 μW.

Table I lists the wavelengths and radiant powers used for each curve in Fig. 5. Also included are the slopes (base 10 logarithm), intercepts, and correlation coefficients that resulted from a linear regression analysis of the data in the region from the forward current offset to attainment of 100% quantum efficiency. Device I was also measured at 676.4 nm; the results are listed in the table but not in Fig. 5.

A number of observations can be made from Fig. 5 and Table I regarding these data. The variation of quantum efficiency due to the recombination trap effect is quite linear with respect to the logarithm of the reverse bias voltage as can be seen from the correlation coefficients which are close to unity. The amount of bias voltage required to offset the forward current is different for each device (i.e., it is photodiode dependent) but is independent of wavelength. The slope of

Table I. Experimental Conditions Used in Generating Fig. 5 and Results of a Linear Regression Analysis

Curve/device	Wavelength (nm)	Radiant power (mW)	Voltage at forward current offset (V)	Intercept	Slope	Correlation coefficient
A/I	406.7	2.2	1.3	—	—	—
B/II	632.8	1.9	3	0.981	0.0177	0.998
C/III	676.4	1.9	10	0.974	0.0155	0.979
D/I	799.3	1.6	1.3	0.900	0.0442	0.999
E/I	799.3	0.016	0	0.870	0.0462	0.996
[a]/I	676.4	2.0	1.3	0.979	0.0153	0.982
[a]/I	676.4	0.017	0	0.976	0.0123	0.989

[a] Curve not shown in Fig. 5.

in a spot 3–4 mm in diameter. At 406.7 nm it was found that, depending on the device, 1–10-V reverse bias was required to offset the forward current due to the high flux density. The forward current effect occurs at all wavelengths, whereas the recombination trap effect occurs only at long wavelengths. To overcome the recombination trap effect at 632.8 nm, 10–20-V reverse bias was required; at 676.4 nm, it was 30 to 40 V; and at 799.3 nm, an extrapolation indicated that ~180 V would be necessary. However, this photodiode would probably have broken down and become conductive before the optimum voltage was reached.

Figure 5 shows the quantum efficiency vs reverse bias at the four wavelengths studied. This is a rather busy figure, but it is included in this form to show several effects that are obvious when the data are examined in this grouping. Table I should also be consulted when examining this figure. Curves *A*, *B*, and *C* were obtained with three different multiple detector devices I, II, and III, respectively. Curves *D* and *E* were obtained with Device I. The differences between the devices is due to the differences among the particular photodiodes used in the devices. Devices I and III used inversion layer photodiodes selected for low dark current at high reverse bias. For Device II, the maximum usable reverse bias was ~17 V. No information was available regarding fabrication differences among the various photodiodes used.

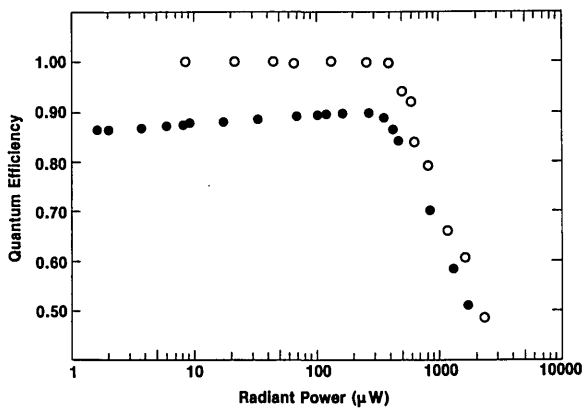

Fig. 6. Measured quantum efficiency as a function of radiant power level at 406.7 nm ○ and 799.3 nm ●.

the linear region is wavelength dependent. The amount of bias voltage required to achieve 100% quantum efficiency is wavelength dependent; higher bias voltages are required at longer wavelengths. Finally, at long wavelengths and low radiant power, higher reverse bias voltages are required to achieve 100% quantum efficiency.

Figure 6 is a plot of the quantum efficiency measured at two wavelengths as a function of the radiant power at zero reverse bias. This plot illustrates both the effect of the saturation nonlinearity and, for the 799.3-nm

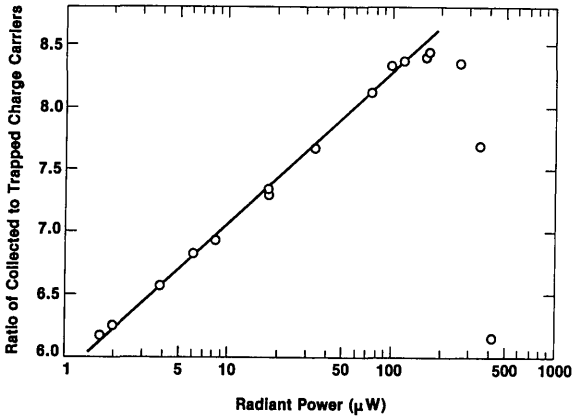

Fig. 7. Ratio of collected to trapped photogenerated charge carriers as a function of radiant power level at 799.3 nm.

data, the supraresponsivity nonlinearity. These effects are more correctly a function of photon density. However, because the actual irradiated area was not precisely known and because the radiation distribution was not uniform, the data are plotted simply as a function of radiant power. The scatter in the 406.7-nm data at the higher power levels is probably due to day to day variations in spot size, beam uniformity, and position on the detector surface. At 799.3 nm these conditions were under better control. In the 1–100-μW radiant power range the quantum efficiency at 799.3 nm is observed to be linearly related to the logarithm of the radiant power. The slope (base 10 logarithm) and intercept obtained from a linear regression analysis are 0.0177 and 0.857, respectively.

The quantum efficiency is the ratio of the number of charge carriers collected N_c to the total number generated. Therefore,

$$N_c/N_t = Q/(1 - Q), \tag{4}$$

where N_t is the number of trapped carriers. As shown in Fig. 7, the ratio of collected-to-trapped minority charge carriers is also linearly related to the logarithm of the radiant power. Fitting a straight line to these data yields a slope (base 10 logarithm) and intercept of 1.20 and 5.86, respectively. The ratio of collected-to-trapped minority carriers can be expected to reach a constant minimum (nonzero) value at low radiant power levels.[9] Since the data in Fig. 7 obviously show no sign of leveling off, these measurements are not at a low enough power level to have reached constant quantum efficiency.

As with all diodes, application of a reverse bias to a silicon photodiode causes the dark current to increase. The detailed behavior of the dark current vs bias voltage is, of course, different for different photodiodes. As a class, however, one may reasonably expect an inversion layer photodiode to behave like an n-p rather than a p-n photodiode. This is shown in Fig. 8 where the dark current vs reverse bias voltage is shown for three types of silicon photodiode. The inversion layer type is shown by curves B and D, the phosphorus doped n-p type by curves C and E, and the boron doped p-n type by curves A, F, and G. The photodiodes used in two of the three multiple detector devices studied were selected for low dark current at high reverse bias represented by curve D; the other one had a dark current behavior represented by curve B. The difference in the dark current between the p-n and the n-p type of photodiode is most likely due to leakage current along the SiO_2–Si interface and out to the edges of the chip. In the p-n photodiodes, the positive charge layer in the SiO_2 repels the majority charge carriers away from the interface thereby impeding the reverse current. A guard ring on the n-p and inversion layer photodiodes would have a similar effect and might produce a substantial reduction in the dark current. Curve A is included to show that some p-n photodiodes can have very high dark current under reverse bias. This photodiode would not be suitable for many radiometric applications. At zero reverse bias the dark current of the four inversion layer photodiode devices used in this study was found to be $<5 \times 10^{-12}$ A. This was measured at a gain of 10^7 A/V and in fact may not be the fundamental noise limit for these devices but simply a residual offset in the electronics used in this study.

It is interesting that none of these photodiodes behaves like an ideal solid state diode.[16] In the ideal case, one would expect a saturation of reverse current with increasing voltage until the breakdown voltage was reached. For all the diodes depicted in Fig. 8 the resistance in parallel with the junction is apparently too low.

IV. Discussion

The light-trapping arrangement of four inversion layer photodiodes described above is the first 100% efficient quantum detector. That is, one incident photon produces one electron in the external circuit under a wide variety of use conditions. It was demonstrated that at laser power levels of the order of a milliwatt and wavelengths ranging from 407 to 676 nm, the quantum efficiency was 0.999 to within ±0.2%. For one device that could be operated at 100-V reverse bias, the external quantum efficiency at 800 nm was still within 1% of unity.

There is no reason to believe that 2 mW is the upper limit for these devices. This is an aspect that needs to be investigated.

As the probability of photon penetration beyond the depletion region increases (i.e., at long wavelengths), the collection efficiency falls below unity. This can be overcome, but because the reverse voltage leads to an increase in the dark current, the lowest measurable radiant power is limited and is, therefore, a function of wavelength. If a reasonable signal level is assumed to be a factor of 10 above the dark current, for Device I the lowest accurately measurable power at 676 nm is of the order of 10 μW, and at 407 nm it would be ~0.1 nW. Long integration times and precise dark current measurements would, of course, enable one to obtain accurate measurements at lower power levels. Alternatively, it may be possible to use chopped radiation and

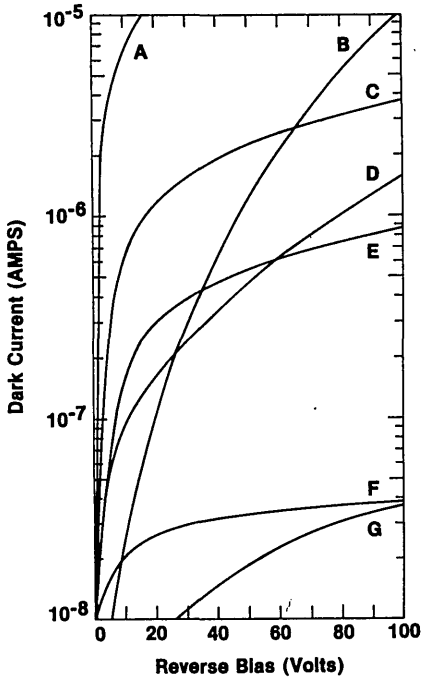

Fig. 8. Dark current vs reverse bias voltage for several different types of silicon photodiode: *A,F,G*, UV-enhanced boron doped *p-n* type; *B,D*, inversion layer (undoped) type; *C,E*, phosphorus doped *n-p* type. All are without guard rings.

a lock-in amplifier to make measurements at lower power levels. For optimum accuracy, the gain of the lock-in would, of course, have to be calibrated.

Selecting the optimum reverse bias voltage for the wavelength and power level of interest is simply a matter of measuring the output as a function of increasing bias voltage. Attainment of constant output indicates that sufficient bias has been applied. No bias is required at short wavelengths and low radiant power levels.

Because the variation of quantum efficiency with reverse bias (Fig. 5) and with radiant power (Fig. 6) and the variation of the ratio of collected-to-trapped carriers with radiant power (Fig. 7) all appear to be simple relationships, one is tempted to speculate on a possible model to fit these observations. However, such digression is beyond the scope of this paper. Further studies of these phenomena, especially on the *p-n* type of photodiode about which so much is already known,[2,9,17,18] may prove quite fruitful.

In the blue region of the spectrum the devices studied were polarization sensitive. This can be an advantage since the quantum efficiency for one polarization (TM mode) is very close to unity. The largest deviation is at 365 nm, where the calculated quantum efficiency is 0.996 vs 0.982 for unpolarized light. In a polarized beam, rotating the device about the optic axis to maximize the output assures nearly unit quantum efficiency from 350 on out to ~700 nm. One could, of course, use the predicted quantum efficiency in Fig. 4 as a nominal correction factor in the 350–450-nm spectral region. Such a correction can be made with a reasonable degree of accuracy. For example, if the nominal curves in Fig. 4 are assumed to deviate from the true value by not more than 10%, for unpolarized radiation a correction based on these curves would be in error by at most 0.2% at 365 nm. Rather than assume a correction based on nominal reflectance, one can, of course, measure the reflectance of the first photodiode *in situ* and determine a more accurate correction for the device at hand.

Besides being an extremely accurate and simple laser power meter the devices described above should have many uses in radiometry, especially if a substantial improvement can be made in the field of view of these devices. An obvious improvement would be to have a tighter packing and/or an enlargement of the active area of the silicon photodiodes. In the devices used in this work, the minimum packing distance was determined by the size of the header in which the photodiodes are commonly mounted. It is a simple matter to reduce the header dimensions; however, an enlargement of the active area of the photodiode requires a considerable but not impossible change in the manufacturing process.

Another improvement would be to eliminate the polarization sensitivity by rotating successive detectors so that the plane of reflection is changed by 90° relative to the preceeding reflection. That is, the TM mode for the first detector would be TE at the second, TM at the third, and so on. To be completely polarization insensitive an odd number of detectors is required: pairs of 45° incident detectors plus one detector at normal incidence. As successive rotated pairs of detectors are added to the chain, the optical path would take on the appearance of a spiral made up of right angle turns.

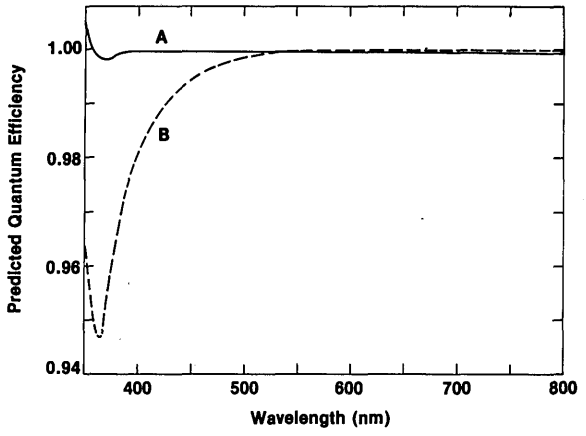

Fig. 9. Predicted quantum efficiency of a three-detector spiral configuration light-trapping device showing the effect of two different thicknesses of SiO_2: *A*, 70 nm; *B*, 140 nm.

The minimum number of detectors for a polarization insensitive device is three. Such a device has the advantage of a much bigger acceptance angle than the tightly packed four-detector device. However, it would have the disadvantage of a much larger deviation from 100% quantum efficiency in the blue and near UV spectral region. An obvious improvement would be to change the thickness of the SiO_2 layer so as to minimize the reflectance in the blue and near UV spectral region. It was found that the 45 and 0° reflectances at 365 nm were minimized with a 60–80-nm thick SiO_2 layer, while at the same time yielding acceptably low reflectance levels in the rest of the spectrum. Figure 9 shows the predicted quantum efficiency of the three detector spiral device for two thicknesses of SiO_2. For 70-nm thick SiO_2 the predicted quantum efficiency is within 0.2% of unity below 400 nm and within 0.04% throughout the rest of the spectrum. Changing the thickness of the SiO_2 layer will require a considerable, but not impossible, change in the manufacturing process. It may be that a decrease of the thickness of the SiO_2 layer will adversely affect the reverse bias voltage limit so that long-wavelength measurements with thin SiO_2 layer photodiodes may be impossible. One can, of course, have different devices tailored for optimum performance in different spectral regions.

It may prove to be impossible to improve substantially the long-wavelength performance of inversion layer photodiodes even with a thicker SiO_2 layer. A possible alternative is to use a *p-n* type of silicon photodiode that can be fully depleted at a high reverse bias. In this case one now has to contend with the collection efficiency losses at the SiO_2–Si interface. One possible solution is to use the corona-discharge method[19] to bring the collection efficiency in this region up to 100%. This requires that a corona-discharge electrode be designed to fit in the frame holding the photodiodes (but out of the light path) so that the photodiode surface can be continually refreshed with electrons. Alternatively, the *p-n* photodiode could be modified as suggested in Ref. 19 by putting a second ring-shaped electrode within the ring-shaped anode. A small voltage constantly applied to the second electrode would prevent the leakage of the static charge from the surface so that the photodiode surface need be only infrequently refreshed with electrons.

References

1. E. F. Zalewski and J. Geist, Appl. Opt. **19,** 1214 (1980).
2. J. Geist, E. F. Zalewski, and A. R. Schaefer, Appl. Opt. **19,** 3795 (1980).
3. C. G. Hughes III, Appl. Opt. **21,** 2129 (1982).
4. J. Geist, J. Appl. Phys. **51,** 3993 (1980).
5. J. Geist, E. Liang, and A. R. Schaefer, J. Appl. Phys. **52,** 4879 (1981).
6. T. E. Hansen, Phys. Scr. **18,** 471 (1978).
7. J. B. Fowler, M. A. Lind, and E. F. Zalewski, Natl. Bur. Stand. U.S. Tech. Note 987 (1979).
8. J. Geist, L. B. Schmidt, and W. E. Case, Appl. Opt. **12,** 2273 (1973).
9. A. R. Schaefer, E. F. Zalewski, and J. Geist, Appl. Opt. **22,** 1232 (1983).
10. W. Budde, Appl. Opt. **18,** 1555 (1979).
11. W. Budde, Appl. Opt. **21,** 3699 (1982).
12. M. Born and E. Wolf, *Principles of Optics* (Pergamon, London, 1965), p. 632.
13. H. R. Philipp, J. Appl. Phys. **43,** 2835 (1972); and private communication.
14. I. H. Malitson, J. Opt. Soc. Am. **55,** 1205 (1965).
15. F. J. Wilkinson, A. J. D. Farmer, and J. Geist, J. Appl. Phys. **54,** 1172 (1983).
16. A. S. Grove, *Physics and Technology of Semiconductor Devices* (Wiley, New York, 1967), p. 150.
17. J. Geist and E. F. Zalewski, Appl. Phys. Lett. **35,** 503 (1979).
18. J. Geist, W. K. Gladden, and E. F. Zalewski, J. Opt. Soc. Am. **72,** 1068 (1982).
19. J. Geist, A. J. D. Farmer, P. J. Martin, F. J. Wilkinson, and S. J. Collocott, Appl. Opt. **21,** 1130 (1982).

The authors wish to thank Jon Geist of NBS for use of the computer program to calculate reflectance and for many fruitful discussions and Warren Gladden of NBS for assistance with some of the measurements.